REMOVAL OF METHYLENE BLUE FROM INDUSTRIAL EFFLUENTS USING CORNCOB ACTIVATED CARBON

ABSTRACT

Water contamination by methylene blue (MB) is a threat to human health and aquatic biota due to its toxicity, persistence, and non-biodegradability. However, there is little data available in the literature on the methylene blue removal approach from industrial effluents by corncob-activated carbon. The purpose of this study was to investigate the adsorption of methylene blue from aqueous solution and industrial effluents by corncob-activated carbon. The methylene blue adsorption capacities of corncob-activated carbon were investigated by batch adsorption experiments both in synthetic solutions and industrial effluents. The optimum pH value was 10.3 with a removal percentage of 93.4 %. Methylene blue adsorption by activated carbon followed second-order kinetics and was well fitted by the Langmuir model. The maximum adsorption capacity (Qmax) value was 11.36 mg/g. This study revealed that corncob-activated carbon has successfully removed methylene blue from industrial effluents, with percentages ranging from 65.14 %, and 76.28 %. The excellent methylene blue dye removal efficiency with corncob activated from industry effluents suggests its promising potential in remediating methylene blue contaminated wastewater.

Keywords: Methylene blue, adsorption, activated carbon, industrial effluents

1. INTRODUCTION

"Water contamination by dyes is a global concern due to their negative effects on human health and the aquatic environment" [1]. For example, the presence of dye in the aquatic environment reduces light penetration, which negatively affects photosynthesis [2, 3]. Therefore, it is important to remove dyes from wastewater.

Methylene blue is commonly used in many fields such as cosmetics, textile, food, pharmaceutical, and paper industries [4, 5]. Methylene blue ingestion by Humans even at low concentrations causes skin cancer, mental confusion, and high blood pressure [4]. However, methylene blue removal from wastewater is important. Thus, several methods such as filtration, electrocoagulation processes, oxidation, and adsorption have been developed to treat dyestuffs wastewater [6 - 10]. Among them, "the adsorption technique is well used due to its simple operation conditions and chemical removal efficacy. The adsorption method has been carried out using several adsorbents such as metal oxides, chitosan, graphene, graphene oxides, and activated carbons" [11 - 15]. To reduce the water treatment price, adsorbents from agricultural byproducts were used by many researchers [16 - 20]. These studies have shown that activated carbons developed from agricultural byproducts effectively

remove methylene blue from aqueous solutions. In addition, these investigations did not focus on industrial effluents. Recently, Kouassi et al. [21] showed that corncob-activated carbon successfully removed Cu^{2+} and Pb^{2+} ions from industrial effluents. However, there are few studies on methylene blue removal from industrial effluents by corncob-activated carbon. The objectives of this study were : (i) to investigate the influence of pH, contact time, adsorbent mass, and initial methylene blue concentration on methylene blue adsorption corncob activated carbon, and (ii) to explore the feasibility of removing methylene blue from industrial effluents by activated carbon.

2. MATERIALS AND METHODS

2.1. Materials, and reagents,

In this study, the reagents used include methylene blue ($C_{16}H_{18}ClN_3S$), sodium hydroxide (NaOH), and hydrochloric acid (HCl). These reagents were purchased from Merck, Germany. The concentrations of methylene blue in the solutions before and after adsorption were determined using the spectrophotometer HACH DR 6000 at 664 nm. The pH values were measured using a pH meter HANNA HI.9828.

2.2. Preparation of activated carbon

The corncob-activated carbon used in the present study was the best-activated carbon prepared by Kouassi et al. [21]. The activated carbons were prepared to take into account the impregnation ratio which is defined as the ratio of the H_3PO_4 weight to the dried corn cob weight. The impregnation ratios were 0.25, 0.5, 1, 1.5, and 2. The mixture of H_3PO_4 and corncob was stirred for 24 h. After impregnation, corn cobs were dried in an oven at 80 °C for 24 h and were carbonized at 500 °C for 2 h in an electric furnace (Advantech KL-280).

2.3. Scanning Electron Microscopy (SEM)

The textural morphology of the best-activated carbon was determined using scanning electron microscopy (SEM) [21].

2.4. pH at the point of zero charge (pH_{pzc})

The pHpzc of activated carbon was determined in the previous study of Kouassi et al. [21]. Various solutions of 0.01 M NaCl of pH ranging between 2 and 12 were prepared. The pH was adjusted with 0.1 M NaOH or 0.1 M HCl solution. Then, 0.1 g of activated carbon was suspended in 50 mL of 0.01 M NaCl solution and agitated for 48 h. After agitation and filtration of the as-prepared solution, the final pH of the filtrate was measured. The curve of (pH_final-pH_initial) vs.pH_initial was used to determine the value of pHpzc, which is the intercept point of the curve (pH_final-pH_initial) vs.pH_initial with the pH_initial line.

2.5. Adsorption experiments

The adsorption tests were carried out at room temperature. After shaking at 250 rpm, the solutions were filtered using Millex Millipore of 47 mm pore size before analyses.

2.5.1. Batch adsorption in aqueous solution

In the aqueous solution, the effect of contact time, pH, activated carbon dose, and initial methylene blue concentration were carried out. To study the effect of contact time, 1g of corncob-activated carbon was added into 200 mL of 10 mg/L of methylene blue solution. The suspension was stirred at 25°C. At various time intervals (5 min, 10 min, 15 min, 30 min, 45 min ,60 min, 90 min, 120 min, 150 min et 180 min) 5 mL was collected. The isotherm experiments were investigated by the varying initial concentration of methylene blue from 10 to 100 mg/L. The activated carbon mass of 0.2 g was added in methylene blue solutions. The suspensions were continuously stirred for the equilibrium time (45 min). To investigate the effect of activated carbon mass, the initial concentration of methylene blue (10 mg/L) and agitation time (45 min) were set at their optimum values. The experiment was done using 20 mL solutions of 10 mg/L of methylene blue for the various adsorbent masses 0.1, 0.3, 0.4, 0.5, 0.6 g, 0.7 g and 0.8g. The effect of pH was carried out by setting the concentrations of methylene blue and activated carbon mass at their optimum values of 10 mg/L and 0.4 g, respectively, and varying the pH from 2 to 11. The adsorption percent was calculated as follows :

$$\% \, \mathbf{Ads} \, = \frac{(C_0 - C_e) \times 100}{C_0} \tag{1}$$

Where C_0 (mg/L), and C_e (mg/L) are the initial, and the equilibrium concentrations of methylene blue, respectively.
The methylene blue amount adsorbed by the activated carbon at time t was determined using the following relationship :

$$\mathbf{q_t} \, = \frac{(C_0 - C_t) \times V}{m} \tag{2}$$

In this equation, C_t (mg/L) represents the dye concentration in the solution after a contact time t (min), C_0 (mg/L) the initial concentration, V (L) the volume of the solution, and m (g) the mass of the activated carbon.

At the equilibrium, the amount of dye adsorbed was calculated as follows :

$$\mathbf{q_e} \, = \frac{(C_0 - C_e) \times V}{m} \tag{3}$$

Where C_0 (mg/L) and C_e (mg/L) are the initial and equilibrium dye concentrations, respectively; V(L) is the volume of solution, and m (g) is the activated carbon mass

2.5.2. Adsorption experiment with industrial dye effluents

The industrial effluent samples were collected around a paint manufacturing industry (sample 1) and a textile industry (sample 2) in Abidjan City which is the biggest town in Côte d'Ivoire.

3

0.4 g of activated carbon was added to 20 mL of sample 1 or sample 2. The suspensions were continuously agitated for 2 hours at room temperature.

2.6. Kinetic and isotherms models

2.6.1. Kinetic models

In this study, various models such as pseudo-first-order [22] and pseudo-second-order [23], were used to understand the kinetic adsorption of methylene blue.

Equation (4) gives the expression of the nonlinear form of the pseudo-first-order model :

$$\mathbf{q_t = q_e[1 - \exp(-k_1 t)]} \qquad (4)$$

Where k_1 (min^{-1}) represents the rate constant of the pseudo-first-order, q_t (mg/g) and q_e (mg/g) are the amounts of methylene blue adsorbed at time t (min) and equilibrium time, respectively.

For the pseudo-second-order model, the following equation gives the expression of nonlinear form.

$$\mathbf{q_t = \frac{q_e^2\, k_2\, t}{1 + q_e\, k_2\, t}} \qquad (5)$$

In these equations, k_2 (g. mg^{-1}.min^{-1}) represents the rate constant of the pseudo-second-order model

2.6.2. Adsorption isotherm models

In this study, the experimental data of adsorption isotherms were described by Langmuir [24] and Freundlich [25] adsorption models.

Equations (6), and (7) give the expressions of the nonlinear forms of Langmuir and Freundlich adsorption models, respectively :

$$\mathbf{Q_e = \frac{Q_{max} \times K_L \times C_e}{1 + (K_L \times C_e)}} \qquad (6)$$

$$\mathbf{Q_e = K_F \times C_e^{1/n}} \qquad (7)$$

Where C_e (mg/L) is the equilibrium methylene blue concentration; Qe (mg/g) is the amount of methylene blue adsorbed at equilibrium, K_L (L/mg) is the Langmuir constant, K_F is the Freundlich constant, Q_{max} (mg/g) is the maximum adsorption capacity, and, n is the Freundlich model exponent,

The favorability of adsorption is indicated by the Langmuir parameter (R_L) which is calculated as follows :

$$\mathbf{R_L = \frac{1}{1 + b \times C_0}} \qquad (8)$$

Where C_0 is the highest initial solute concentration. $R_L < 1$ indicates unfavorable adsorption, the adsorption is favorable when $0 < R_L < 1$, and the adsorption is irreversible when $R_L = 0$

2.6.3. Error analysis

To find the best nonlinear model, an error analysis was performed. The Sum of Squares Errors (SSE), and the Chi-square (χ^2) were achieved by the following equations :

$$SSE = \sum_{i=1}^{n}(q_{e\ exp} - q_{e\ cal})^2 \tag{9}$$

$$\chi^2 = \sum_{i=1}^{n}\frac{(q_{e\ exp} - q_{e\ cal})^2}{q_{e\ cal}} \tag{10}$$

Where $q_{e\ exp}$ and q_{ecal} are experimental and predicted adsorption capacities, respectively.

3. RESULTS AND DISCUSSION

3.1. Properties of Activated Carbon

The properties of corncob-activated carbon such as specific surface area (Table 1), surface morphology (Figure 1), and pH at the point zero charge (pH$_{PZC}$) of corncob-activated carbon have been previously reported by Kouassi et al. [21]. The maximum value of the specific surface area of 810 m^2/g was obtained for an impregnation ratio of 1. The results also showed a porous structure of activated carbon at impregnation ratio 1 (figure 1). The value of the pH at the zero point charge (pH$_{PZC}$) of the activated carbon at impregnation ratio 1 was 3.8.

Table 1 Effect of different impregnation ratios on the surface area of activated carbon

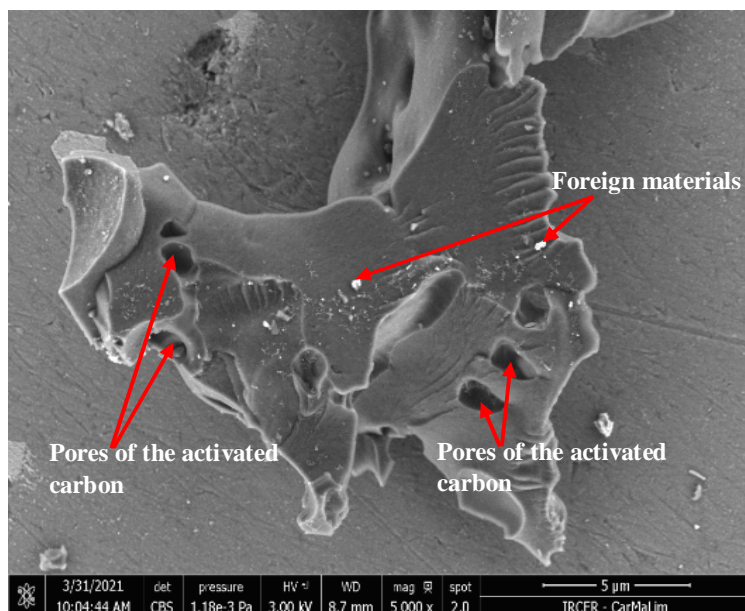| Impregnation ratio	Specific surface area S (m^2/g)
0	184
0.25	717
0.5	779
1	810
1.5	502
2	306

SEM image of activated carbon at impregnation ratio 1

3.2. Effect of contact time on adsorption efficiency and kinetic study in aqueous solution

The influence of contact time on methylene blue adsorption is shown in figure 2. The results showed that the adsorption of methylene blue was very rapid during the first 5 min and slow near the equilibrium. This behavior is due to the large number of sites available at the beginning of the process, which are occupied throughout the process, making the diffusion of methylene blue difficult [26]. The adsorption equilibrium was reached at 45 min with a maximum adsorption capacity of 1.98 mg/g. The pseudo-first-order, and pseudo-second-order, models were applied to understand the methylene adsorption mechanism. The results are shown in figure 3 and table 2. Comparing the Chi-Square (χ^2), the sum of error squares (SSE), and the coefficient of determination (R^2) values, the pseudo-second order was found to control methylene blue adsorption. Indeed, (χ^2), and SSE values obtained with pseudo-second-order were lower than those of pseudo-first order. In addition, the R^2 value with pseudo-second-order was higher than that of the pseudo first order. Moreover, the results of the pseudo-second model (Table 2) revealed that the maximum adsorption capacity obtained theoretically (Qe_2 theo = 1.98 mg/g) are close to those obtained experimentally (Qe exp = 2.08 mg/g).
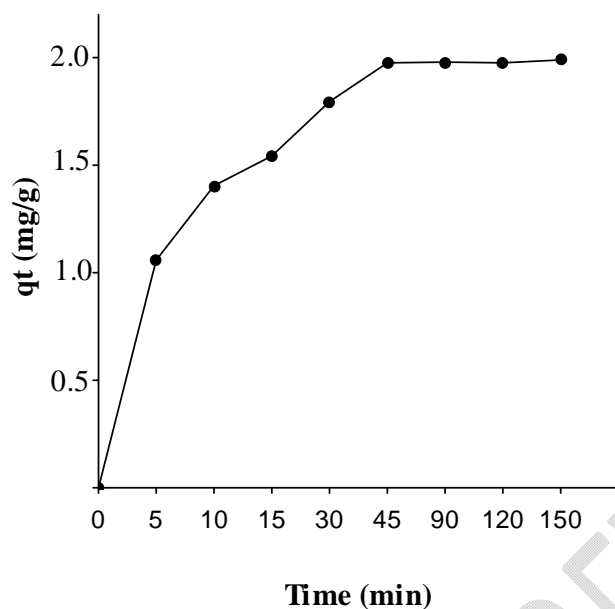
Fig. 2. Effect of contact time on adsorption capacities of methylene blue
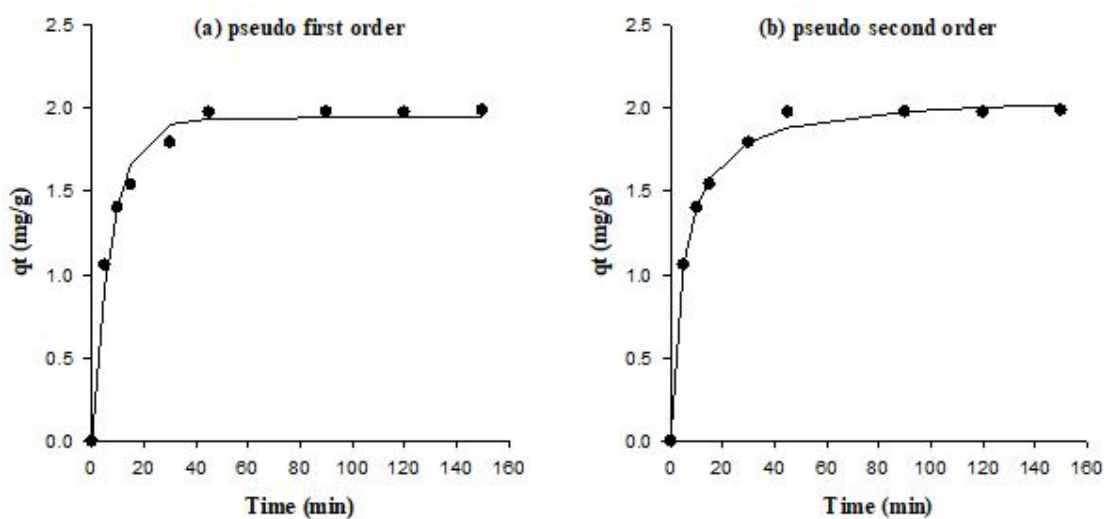

Fig. 3. Adsorption kinetics: (a) nonlinear pseudo-first-order model and (b) nonlinear Pseudo-second-order model for removal of methylene blue

Table 2. Parameters of pseudo-first-order, pseudo-second-order, Langmuir, and Freundlich models using nonlinear analysis

		Qe exp (mg/g) : 1.98	
Kinetic	**Pseudo first order**	Qe_1(mg/g)	1.94
		k_1	0.13
		χ^2	0.04
		SSE	0.05
		R^2	0.984
	Pseudo second order	Qe_2(mg/g)	2.08
		k_2	0.09
		χ^2	0.006
		SSE	0.011
		R^2	0.996
Isotherm	**Langmiur**	Qmax(mg/g)	11.36
		K_L	0.27
		R_L	0.04
		χ^2	0.55
		SSE	2.13
		R^2	0.97
	Freudlich	K_F	2.77
		n	2.06
		χ^2	0.91
		SSE	3.52
		R^2	0.94

3.3. Effect of adsorbent mass on methylene blue removal in aqueous solution

The percentage removal of methylene blue increased with the mass of adsorbents (figure 4). This observation can be explained by the increase in active sites of activated carbon. The maximum adsorption percentage of methylene blue was 98.8 %, with an activated carbon mass of 0.4 g. Therefore, an activated carbon mass of 0.4 was used for further experiments.
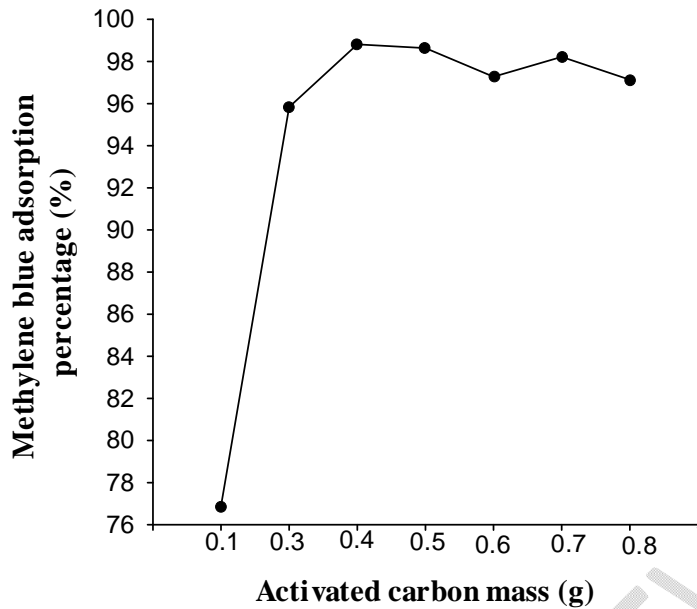
Fig. 4 Effect of activated carbon mass on methylene blue adsorption

3.4. Adsorption capacity of methylene blue in aqueous solution

"The results of the influence of methylene blue initial concentration on methylene blue adsorption are shown in figure 5. The adsorption percentages of methylene blue decreased with increasing initial concentrations due to the reduction of the active sites of activated carbon" [21, 27]. The maximum adsorption percentage (97.4 %) was obtained with an initial concentration value of 10 mg/L. The adsorption isotherms of methylene blue onto activated carbon are shown in figure 6. The adsorbed amounts of methylene blue increase with increasing equilibrium concentration, indicating that the activated carbon exhibited good adsorption capacity to methylene blue. The isotherm adsorption data were fitted by nonlinear forms of Langmuir and Freundlich models (Figure 6 and Table 2). The results indicated that the R^2 value obtained with the Langmuir model (0.97) was higher than that of the Freundlich model (0.94). In addition, the Langmuir SSE and χ^2 values were the smallest. Therefore, methylene blue adsorption isotherm was well described by the Langmuir model, thereby indicating a monolayer adsorption process [27]. In addition, the value of $R_L = 0.04 < 1$ showed that methylene blue adsorption on corncob-activated carbon was favorable. The maximum adsorption capacity (Qm) was 11.36 mg/g, indicating that corncob-activated carbon could be a promising methylene blue adsorbent.

The maximum adsorption capacity (Qm = 11.36 mg/g) of methylene blue obtained in the present study was compared to those of some authors (Table 3). It was found that Qm 11.36 mg/g obtained in this study was higher than those obtained by Aboua et al. [28], Chandra et al. [29], and Sharma and Uma [30]. Whereas, data obtained by Gurer et al. [31], and by

Abdulhameed et al. [32], were higher than the ones found in the current study. Therefore, corncob-activated carbon has obvious advantages compared with some materials in Table 3.
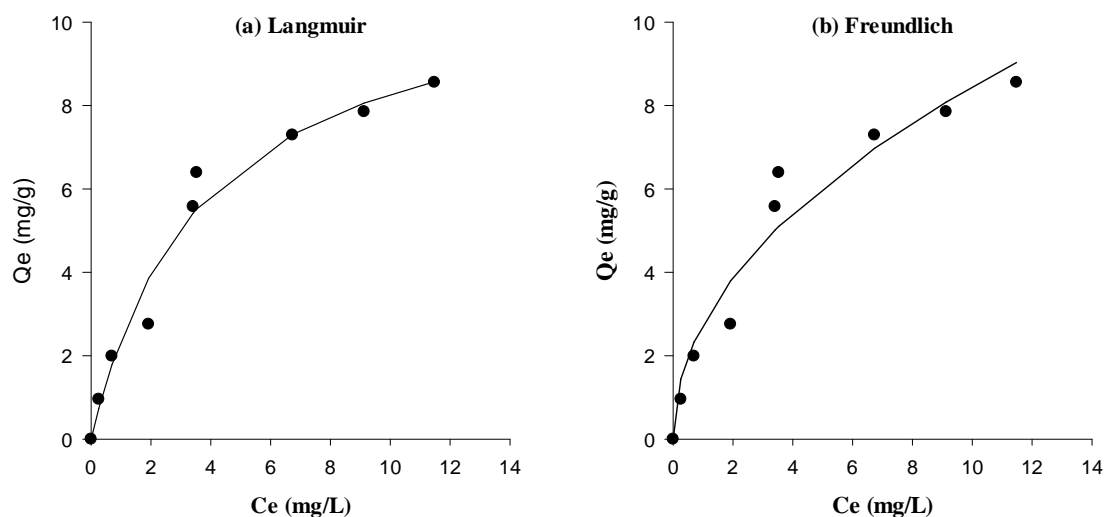
Fig. 5. Effect of initial concentration

Fig. 6 Adsorption isotherms:(a) nonlinear Langmuir isotherm and (b) nonlinear Freundlich isotherm for methylene blue adsorption

Table 3. Comparison of adsorption capacities of different adsorbents for methylene blue removal

Adsorbents	Adsorption capacity Q (mg/g)	References
Macore fruit shells	6.85	[28]
Leaginous microalga,S	7.80	[29]
Rice husk	9.83	[30]
Orange peels	98.9	[31]
Bamboo chip	305.3	[32]
Corncob	11.36	Present study

3.5. Effect of pH on methylene blue adsorption in aqueous solution

Figure 7 showed the results of the influence of pH on the adsorption of methylene blue. The results indicated that the adsorption rates increased up to the optimum pH of 10.3. Above this value, the adsorption rates decrease. Therefore, the adsorption of methylene blue on the activated carbons depends on the aqueous solution pH. The pH optimum value (10.3) was higher than the pH_{pzc} value (3.8). At this pH (10.3) the corncob-activated carbon surface becomes negative. Hence, there was an electrostatic attraction between the negatively charged activated carbon and methylene blue which is a cationic dye (($C_{16}H_{18}N_3Cl^-)S^+$). That can explain the higher percentage removal of methylene blue.
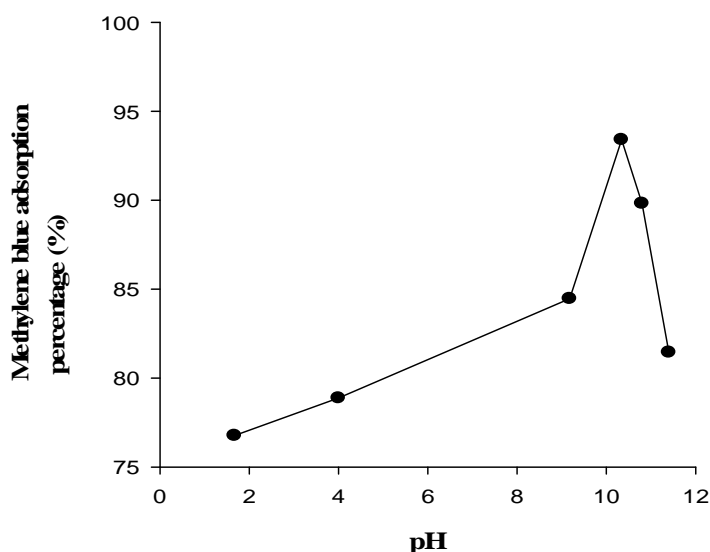

Fig. 7. Effect pH on adsorption capacities of methylene blue

3.6. Methylene blue adsorption mechanism onto activated carbon

Figure 8 shows the adsorption mechanism for methylene blue. Dye adsorption relies on several influential factors such as solution pH, pH of the point zero charge (pHpzc), surface functional groups, and surface characteristics of the adsorbent [33, 34]. Methylene blue is a cationic dye, hence it adsorbs onto activated carbon via electrostatic interaction, hydrogen bonding, π-π interaction, and pore diffusion mechanism [33]. The negative charge of activated carbon favors methylene blue attraction by electrostatic interaction. The pH at the zero point charge (pHpzc) of activated carbon was 3.8. At pH > pHpzc (3.8), the surface of activated carbon was covered with negatively charged hydroxyl (OH^-) and carbonyl ($-COO^-$) groups which electrostatically interact with positively charged (S^+ and N^+ atoms) groups of methylene blue. Several authors such as Kataria et al. [33], Thomas et al. [34], Benjelloun et al. [35], Ramutshatsha-Makhwedzha et al. [36], and Xia et al. [37] reported similar observations for methylene blue at higher pH. The corncob-activated carbon is a carbonaceous material having an organic aromatic structure with a C=C bond π-system. The

π electrons present in the aromatic ring of activated carbon interact with π electrons in the benzenic ring of methylene blue by π-π interaction. Hydrogen bonding is also involved in methylene blue adsorption onto corncob-activated carbon. At pH < pHpzc (3.8), the water molecules and carboxyl (-COO$^-$) groups onto the activated carbon surface may be offered H$^-$ atoms to induce hydrogen bonding with polar S$^-$ or N$^-$ atoms of methylene blue. At basic pH, hydrogen bonding contribution is relatively less as compared to electrostatic interaction. Indeed, methylene blue adsorption percentage (93.4 %)onto corncob-activated carbon was high at basic pH (10.3). The SEM images indicated the porous structure of carbonaceous activated carbon material, thereby indicating the possibility of methylene blue adsorbed via pore diffusion or filling as ⋯ ⋯s the physical process also [33].
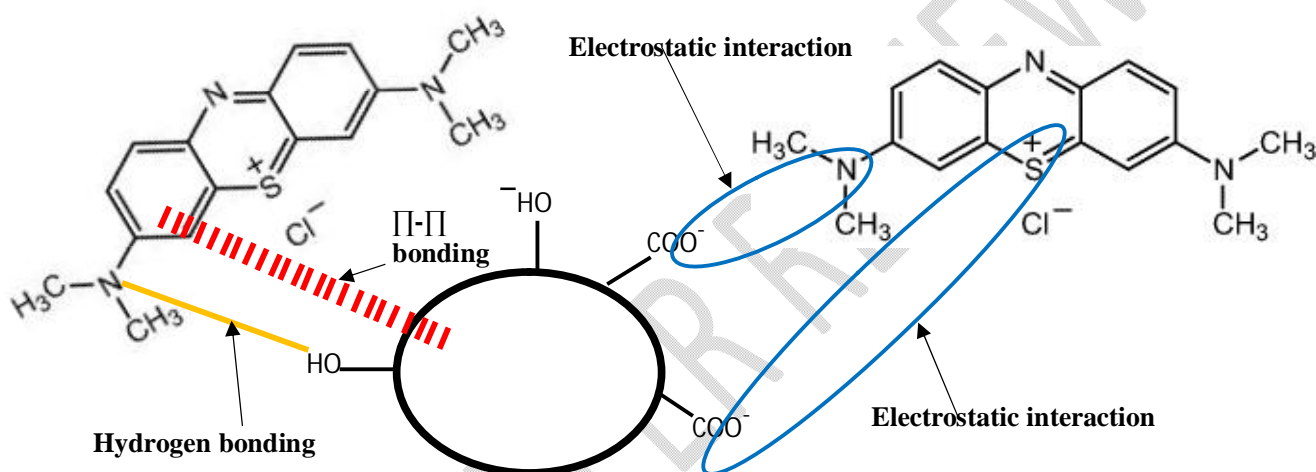

Fig. 8. **Possible interaction and mechanism of methylene blue dye adsorption**

3.7. Adsorption of methylene blue in industrial wastewaters

Table 4 gives the removal percentages of methylene blue from industrial effluents, and from synthetic aqueous solutions. The removal percentages of methylene blue by corncob activated carbon were 76.28 % and 65.14 % for sample 1 and sample 2, respectively. These results showed that methylene blue adsorption percentages decreased in real effluents as compared to methylene blue synthetic solution (98.81 %). The decrease in methylene blue removal from real effluents can be explained by the competition effects between methylene blue and other pollutants present in industrial effluents [38]. Thus, corncob-activated carbon may be proposed to purify real effluents contaminated by methylene blue.

Table 4. Industrial effluents treatment

Sample	Before adsorption (mg/L)	After adsorption (mg/L)	Removal percentage (%)
Methylene blue synthetic solution	10	0.12	98.81
Sample 1	2.53	0.6	76.28
Sample 2	4.02	1.40	65.14

4. CONCLUSION

In the present study, methylene blue removal from aqueous solution and industrial effluents was performed using corncob-activated carbon. In synthetic aqueous solution, the adsorption tests indicated that pH, adsorbent mass, and methylene blue concentration affected methylene blue removal. The optimum pH value was 10.3 with a removal percentage of 93.4 %. The kinetic study showed that the methylene blue adsorption process was better described by the pseudo-second-order model, indicating that the chemisorption limits the adsorption process. The results also showed that the Langmuir model was the best model to fit methylene blue adsorption data, indicating a monolayer adsorption process. The maximum adsorption percentage in an aqueous solution was 98.81 %. The investigations with industrial effluents indicated that the adsorption percentages of methylene blue by activated carbon varied between 65.14 % and 76.28 %. Therefore, corncob-activated carbon may be proposed to purify real effluents contaminated by methylene blue.

REFERENCES

1. Cheng J, Zhan C, Wu J, Cui Z, Si J, Wang Q, Peng X, Turng LS. Highly Efficient Removal of Methylene Blue Dye from an Aqueous Solution Using Cellulose Acetate Nanofibrous Membranes Modified by Polydopamine. ACS Omega. 2020 ; 5: 5389−5400. https://dx.doi.org/10.1021/acsomega.9b04425

2. Mehra S, Singh M, Chadha P Adverse Impact of Textile Dyes on the Aquatic Environment as well as on Human Beings. Toxicol Int. 2021 ; 28(2): 165-176, https://dx.doi.org/10.18311/ti/2021/v28i2/26798

3. Bulgariu L, Escudero LB, Bello OS, Iqbal M, Nisar J, Adegoke KAA, Alakhras F, Kornaros M, Anastopoulos L. The utilization of leaf-based adsorbents for dyes removal. A review. J Mol Liq. 2019 ; 276 :728–747. https://doi.org/10.1016/j.molliq.2018.12.001

4. Al-Ghouti AA, Sweleh AO. Optimizing textile dye removal by activated carbon prepared from olive stones. Environ Technol Innov. 2019 ; 16: 100488. https://doi.org/10.1016/j.eti.2019.100488

5. Mouni L, Belkhiri L, Bollinger JC, Bouzaza A, Assadi A, Tirri A, Dahmoune F, Mamadi K, Remini H. Removal of Methylene Blue from aqueous solutions by adsorption on Kaolin : Kinetic and equilibrium studies. Appl Clay Sci. 2018 ; 153 : 38–45 https://doi.org/10.1016/j.clay.2017.11.034

6. Assémian AS, Kouassi KE, Drogui P, Adouby K, Boa D. Removal of a Persistent Dye in Aqueous Solutions by Electrocoagulation Process: Modeling and Optimization Through Response Surface Methodology. Water Air Soil Pollut. 2018a ; 229: 184 https://doi.org/10.1007/s11270-018-3813-2

7. Assemian AS, Kouassi KE, Adouby KA, Drogui P, Boa D. Removal of methylene blue in aqueous solutions by electrocoagulation process: Adsorption and kinetics studies. Eur J Chem. 2018b; 9(4) : 311-316. https://doi.org/10.5155/eurjchem.9.4.311-316.1736

8. Han Q, Wang J, Goodman BA, Xie J, Liu Z. High adsorption of methylene blue by activated carbon prepared from phosphoric acid treated eucalyptus residue. Powder Technol. 2020 ; 366: 239-248. https://doi.org/10.1016/j.powtec.2020.02.013

9. Liu X, Chen Z, Du W, Liu P, Zhang L, Shi F. Treatment of wastewater containing methyl orange dye by fluidized three dimensional electrochemical oxidation process integrated with chemical oxidation and adsorption. J Environ Manage. 2022 ; 311 : 114775. https://doi.org/10.1016/j.jenvman.2022.114775

10. Hevira L, Zilfa, Rahmayeni, Ighalo JO, Aziz H, Zein R. Terminalia catappa shell as low-cost biosorbent for the removal of methylene blue from aqueous solutions. J Ind Eng Chem. 2021 ; 97: 188–199. https://doi.org/10.1016/j.jiec.2021.01.028

11. Yu M, Dong H, Zheng Y, Liu W. Ternary metal oxide embedded carbon derived from metal organic frameworks for adsorption of methylene blue and acid red 73. Chemosphere. 2021 ; 280 : 130567. https://doi.org/10.1016/j.chemosphere.2021.130567

12. Vedula SS, Yadav GD. Wastewater treatment containing methylene blue dye as pollutant using adsorption by chitosan lignin membrane : Development of membrane, characterization and kinetics of adsorption. J Indian Chem Soc. 2022 ; 99 : 100263. https://doi.org/10.1016/j.jics.2021.100263

13. Yadav A, Dindorkar SS, Ramisetti SB, Sinha N. Simultaneous adsorption of methylene blue and arsenic on graphene, boron nitride and boron carbon nitride nanosheets: Insights from molecular simulations. J Water Process Eng. 2022 ; 46: 102653. https://doi.org/10.1016/j.jwpe.2022.102653

14. Arabpour A, Dan S, Hashemipour H. Preparation and optimization of novel graphene oxide and adsorption isotherm study of methylene blue. Arab J Chem. 2021 ; 14 : 103003. https://doi.org/10.1016/j.arabjc.2021.103003

15. Gokce Y, Yaglikci S, Yagmur E, Banford A, Aktas Z. Adsorption behaviour of high performance activated carbon from demineralised low rank coal (Rawdon) for methylene blue and phenol. J Environ Chem Eng. 2021 ; 9 (2) : 104819. https://doi.org/10.1016/j.jece.2020.104819

16. Aboua KN, Yobouet AY, Yao KB, Gone DL, Trokourey A. Investigation of dye adsorption onto activated carbon from the shells of Macore fruit. J Environ Manage. 2015 ; 156 :10-14. http://dx.doi.org/10.1016/j.jenvman.2015.03.006

17. Ibrahim M, Souleiman M, Salloum A. Methylene blue dye adsorption onto activated carbon developed from Calicotome villosa via H_3PO_4 activation. Biomass Convers Biorefinery. 2021 ; https://doi.org/10.1007/s13399-021-02027-2

18. Omorogie MO, Babalola JO, Ismaeel MO, McGettrick JD, Watson TM, Dawson DM, Carta M, Kuehnel MF. Activated carbon from Nauclea diderrichii agricultural waste–a promising adsorbent for ibuprofen, methylene blue and CO_2. Adv Powder Technol. 2021 ; 32 : 866–874. https://doi.org/10.1016/j.apt.2021.01.031

19. Medhat A, El-Maghrabi HH, Abdelghany A, Menem NMA, Raynaud P, Moustafa YM, Elsayed MA, Nada AA. Efficiently activated carbons from corn cob for methylene blue adsorption. Appl Surf Sci. 2021 ; 3: 100037. https://doi.org/10.1016/j.apsadv.2020.100037

20. Xue H, Wang X, Xu Q, Dhaouadi F, Sellaoui L, Seliem MK, AB, Belmabrouk H, Bajahzar A, Bonilla-Petriciolet A, Li Z, Li Q. Adsorption of methylene blue from aqueous solution on activated carbons and composite prepared from an agricultural waste biomass: A comparative study by experimental and advanced modeling analysis. Chem Eng. 2022 ; J 430 : 132801. https://doi.org/10.1016/j.cej.2021.132801

21. Kouassi NLB, N'goran KPDA, Blonde LD, Diabate D, Albert T. Simultaneous Removal of Copper and Lead from Industrial Effluents Using Corn Cob Activated Carbon. Chemistry Africa. https://doi.org/10.1007/s42250-022-00432-2

22. Lagergren S. About the theory of so-called adsorption of soluble substances. Kungliga Svenska Vetensk Handl. 1898 ; 24:1–39

23. Ho YS, McKay G. Pseudo-second order model for sorption processes. Process Biochem. 1999 ; 34 :451–465. https://doi.org/10.1016/S0032-9592(98)00112-5

24. Langmuir I. The adsorption of gases on plane surfaces of glass mica and platinum. J Am Chem Soc. 1906 ; 40: 1361–1403. https://doi.org/10.1021/ja02242a004

25. Freundlich HM. Über die adsorption in lösungen.Z. PhysChem-Frankfurt 57A: 1906 ; 385-470.

26. Brito MJP, Veloso CM, Santos LS, Bonomo RCF, Fontan RDCI. Adsorption of the textile dye Dianix® royal blue CC onto carbons obtained from yellow mombin fruit stones and activated with KOH and H_3PO_4: kinetics, adsorption equilibrium and thermodynamic studies. Powder Technol. 2018 ;339 : 334-343. https://doi.org/10.1016/j.powtec.2018.08.017

27. N'goran KPDA, Diabaté D, Yao KM, Kouassi NLB, Gnonsoro UP, Kinimo KC, Trokourey A Lead and cadmium removal from natural freshwater using mixed activated carbons from cashew and shea nut shells. Arab J Geosci. 2018 ; 11: 498-510. https://doi.org/10.1007/s12517-018-3862-2

28. Aboua KN, Yobouet YA, Yao KB, Gone DL, Trokourey A. Investigation of dye adsorption onto activated carbon from the shells of Macore fruit. J Environ Manage 2015; 156,10-14. http://dx.doi.org/10.1016/j.jenvman.2015.03.006

29. Chandra, TS, Mudliar, SN, Vidyashankar S, Mukherji S, Sarada R, Krishnamurthi K, Chauhan, VS. Defatted algal biomass as a non-conventional low-cost adsorbent : Surface

characterization and methylene blue adsorption characteristics. Bioresour Technol. 2015 ;184, 395–404. https://doi.org/10.1016/j.biortech.2014.10.018

30. Sharma YC, Uma.. Optimization of parameters for adsorption of methylene blue on a low-cost activated carbon. J Chem Eng Data. 2010 ; 55, 435–439. https://doi.org/10.1021/je900408s

31. Gurer G A, Aktas K, Akcetin M O, Unsar AE, Asilturk, M. Adsorption Isotherms, Thermodynamics, and Kinetic Modeling of Methylene Blue onto Novel Carbonaceous Adsorbent Derived from Bitter Orange Peels. Water Air Soil Pollut. 2021. 232(4). https://doi.org/10.1007/s11270-021-05090-7

32. Jawad A H, Abdulhameed AS Statistical modeling of methylene blue dye adsorption by high surface area mesoporous activated carbon from bamboo chip using KOH-assisted thermal activation. Energy Ecol Environ. 2020.5(6), 456–469. https://doi.org/10.1007/s40974-020-00177-z

33. Kataria N, Garg VK. Application of EDTA modified Fe_3O_4/sawdust carbon nanocomposites to ameliorate methylene blue and brilliant green dye laden water. Environ Res. 2019 ; 172 : 43–54. https://doi.org/10.1016/j.envres.2019.02.002

34. Thomas P, Rumjit NP, Lai CW, Johan MRB. EDTA functionalised cocoa pod carbon encapsulated SPIONs via green synthesis route to ameliorate textile dyes - Kinetics, isotherms, central composite design and artificial neural network. Sustain Chem Pharm. 2021. 19 : 100349. https://doi.org/10.1016/j.scp.2020.100349

35. Benjelloun M,·Miyah Y, Bouslamti R, Nahali L, Mejbar F, Lairini S. The Fast⬛Efficient Adsorption Process of the Toxic Dye onto Shells Powders of Walnut and Peanut: Experiments, Equilibrium, Thermodynamic, and Regeneration Studies. Chemistry Africa. 2022 ; 5:375–393. https://doi.org/10.1007/s42250-022-00328-1

36. Ramutshatsha-Makhwedzha D, Mavhungu A, Moropeng LM, Mbaya R. Activated carbon derived from waste orange and lemon peels for the adsorption of methyl orange and methylene blue dyes from wastewater. Heliyon. 2022 ; 8 : e09930. https://doi.org/10.1016/j.heliyon.2022.e09930

37. Xia Y, Yao Q, Zhang W, Zhang Y, Zhao M. Comparative adsorption of methylene blue by magnetic baker's yeast and EDTAD-modified magnetic baker's yeast: Equilibrium and kinetic study. Arab J Chem. 2019 ; 12 : 2448–2456. https://doi.org/10.1016/j.arabjc.2015.03.010

38. Alshabib M, Musa O X, Tanimu A, Abdulazeez I, Alhooshani K, Ganiyu SA. Experimental and DFT investigation of ceria-nanocomposite decorated AC derived from groundnut shell for efficient removal of methylene-blue from wastewater effluent. Appl Surf Sci. 2021 ; 536. 1-13. https://doi.org/10.1016/j.apsusc.2020.147749